Complete *d*-Band Dispersion Relation in Sodium Cobaltates

D. Qian,[1] L. Wray,[1] D. Hsieh,[1] L. Viciu,[2] R. J. Cava,[2] J. L. Luo,[3] D. Wu,[3] N. L. Wang,[3] and M. Z. Hasan[1,*]

[1]*Department of Physics, Joseph Henry Laboratories, Princeton University, Princeton, New Jersey 08544, USA*

[2]*Department of Chemistry, Princeton University, Princeton, New Jersey 08544, USA*

[3]*Institute of Physics, Chinese Academy of Sciences, Beijing 100080, China*

(Received 28 June 2006; published 3 November 2006)

We utilize fine-tuned polarization selection coupled with excitation-energy variation of photoelectron signal to image the *complete* *d*-band dispersion relation in sodium cobaltates. A hybridization gap anticrossing is observed along the Brillouin zone corner and the full quasiparticle band is found to emerge as a many-body entity lacking a pure orbital polarization. At low dopings, the quasiparticle bandwidth (Fermion scale, many-body $E_F \sim 0.25$ eV) is found to be smaller than most known oxide metals. The low-lying density of states is found to be in agreement with bulk-sensitive thermodynamic measurements for nonmagnetic dopings where the 2D Luttinger theorem is also observed to be satisfied.

DOI: 10.1103/PhysRevLett.97.186405 PACS numbers: 71.20.Be, 71.30.+h, 73.20.At, 74.90.+n

Sodium cobaltate ($Na_{1/3}CoO_2 \cdot yH_2O$) is the only known example of an oxide superconductor, besides high T_c cuprates, which is realized in the vicinity of a spin-1/2 Mott state. However, unlike the single band cuprates, the layered cobaltate class Na_xCoO_2 is a prime example of a multiorbital interacting electron system. Observations of superconductivity, magnetic order, spin-thermopower, charge-order, non-Fermi-liquid transport, and many other unusual properties [1–3] have led to an extensive body of theories to model the electron behavior [4–18]. The symmetries proposed for the superconducting order parameter [4–7] critically depend on the orbital character of the bands and the Fermi surface topology. Moreover, a measure of the quasiparticle bandwidth is crucial for the theories of enhanced thermopower and anomalous Hall effect [6,8].

Previous angle-resolved photoemission spectroscopy (ARPES) measurements [9–11] have focused on the Fermi surface topology, Luttinger theorem, and low-energy physics. However, many important issues such as the orbital polarization of the quasiparticles, the *reason* for the sinking of the $e_{g'}$ bands, and the effects of *hydration* have not yet been explored. The experimental map of the Fermi surface (FS) [9–11] of these compounds revealed only one FS. The band associated with the corner pockets predicted in local-density approximation (LDA) [12] was observed to have sunk [10,11] below the Fermi level. Three different intrinsic many-body explanations have been advanced to account for this unusual phenomenon. One scenario argues that the corner pockets sink due to a delicate balance of interorbital *Coulomb correlations* [16,17]. A second scenario [18] suggests that the effect of the *random potential* of the sodium layer leads to a weak localization of the pocket states. Finally, it has been suggested that the *polarization employed* in all previous ARPES studies precludes the detection of the pockets [15]. In this Letter, we report high-resolution measurements of the *complete* *d*-band multiplet, which enables a comparison of the data with theoretical models in the literature.

We have extended the electronic structure determination problem in three regards: First, in order to accurately image the band dispersion over the complete Brillouin zone (BZ) we utilized a range of incident photon energies. Second, we employed two distinct pure polarization settings, namely, the *S* and the *P* scattering geometries. Finally, being equipped with these methods, we studied the effect of hydration on the electronic structure. Spectroscopic measurements were performed with 30 to 90 eV photons with better than 12 to 25 meV energy resolution, and angular resolution better than 0.5% of the Brillouin zone at ALS beam lines 10.0.1 and 12.0.1 using Scienta analyzers with chamber pressures better than 4×10^{-11} torr. A rotatable Scienta analyzer allowed us to work under the *P*-geometry [Fig. 1(c)] or *S*-geometry [Fig. 1(d)] polarization mode or under a mixed but tunable configuration. Carefully grown (by two different methods, flux and traveling solvent floating zone) high-quality single crystals

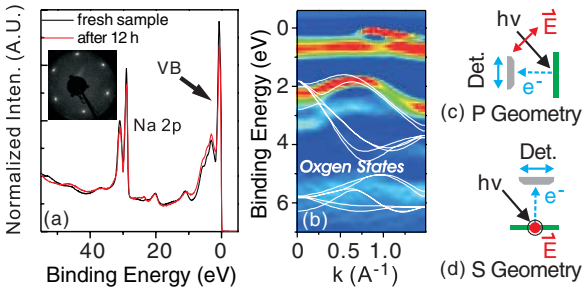

FIG. 1 (color online). Sample characterization: (a) Na-2*p* core level signal is monitored during the experiment. Inset shows the LEED image exhibiting a clear sixfold symmetry of the *in situ* cleaved surface. No ruthenatelike surface reconstruction is observed. (b) No significant shift of the oxygen states are observed at the surface. Experimental configurations employed: Polarization of light is parallel (c) or perpendicular (d) to the plane defined by the sample and the orientation of the detector slits.

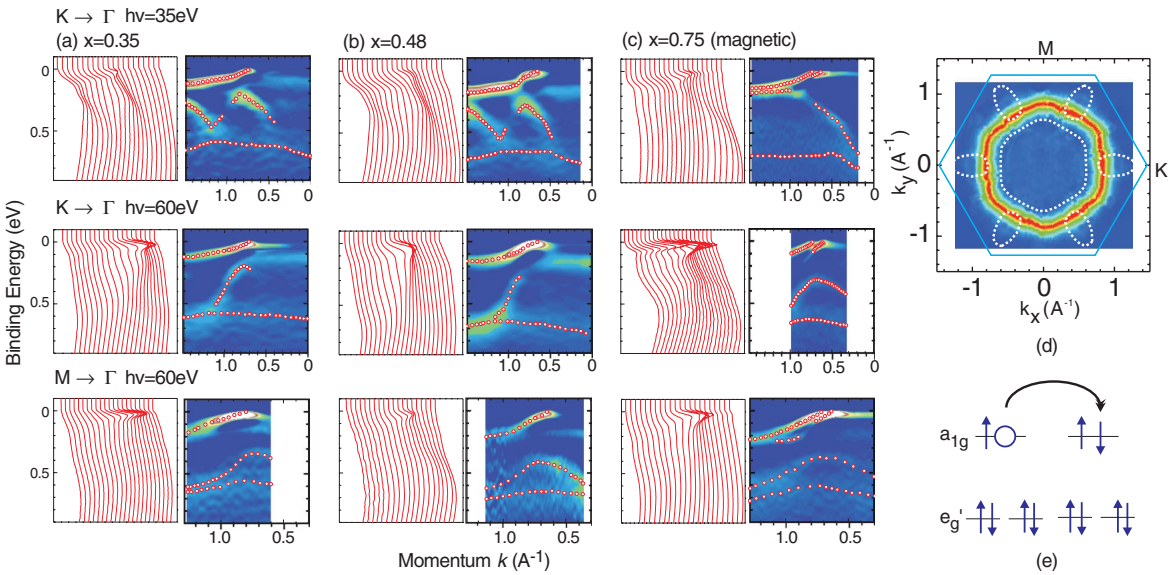

FIG. 2 (color online). Doping evolution of d-band complex: Electron band structures of t_{2g} complex measured along Γ-K (top and middle rows) and Γ-M (bottom row) for doping levels of (a) $x = 0.35$, (b) $x = 0.48$, and (c) $x = 0.75$. Each panel includes energy distribution curves (left) and corresponding secondary derivative image plot (right). The bands are marked using red dots. Bands along Γ-K exhibit strong photon energy dependence. Data for two photon energies are shown: $h\nu = 35$ eV (top) and $h\nu = 60$ eV (middle). No significant photon energy dependence of bands were found along the Γ-M cut. The extended flat feature (unmarked) past the Fermi crossing in image plots for low dopings are due to rapid drop of background. (d) A high-resolution Fermi surface shows that the k-space cuts Γ-K and Γ-M. (e) A cartoon view of hole doping.

over a wide doping range $x = 0.3$, 0.35, 0.48, 0.57, 0.7, and 0.75 were used for this study. Cleaving the unhydrated samples *in situ* at 20 K (or 100 K) resulted in shiny flat surfaces, characterized by electron diffraction to be clean and well ordered with the same symmetry as the bulk [Fig. 1(a)]. The $x = 0.35$ doping was further studied in hydrated ($Na_{1/3}CoO_2 \cdot yH_2O$) and unhydrated ($Na_{1/3}CoO_2$) forms. The hydrated sample surface was prepared by cleaving at 15 K (much below the freezing temperature of H_2O) for the frozen-in retention of hydration. No pressure bursts were observed upon cleaving. Moreover, samples were covered with silver paste to reduce lateral outgassing of H_2O.

Figure 2 shows the doping dependence of band dispersions of the t_{2g} complex measured as a function of incident photon energy. Although a quasiparticle is observed to cross the Fermi level independent of the photon energy or crystal direction used for the measurement, the deeper-lying bands resonate at different photon energies. This sensitivity is remarkable for the high-energy bands, especially along the Γ-K cut. At some photon energies, part of the bands are apparently "missing" or exhibit very small cross section. Therefore to image the full band structure we have explored the bands at many incident photon energies between 30 to 90 eV. The representative data are shown in Fig. 2. Band dispersions are plotted in Fig. 3(a). We note that along all cuts the quasiparticle band that crosses the Fermi level is well separated from the rest. Along the Γ-M cut, there are essentially two branches of the deeper-laying bands. These bands can be traced back to their LDA origin and be labeled as the e_g' bands [12]. With increasing doping they sink below the Fermi level in a systematic way and never cross each other except meeting or emanating from the Γ point. Along the Γ-K cut, a nearly flat band is observed around 0.6 eV. Then in between there is an undulatory band with peak near $k \sim 0.55\pi$. The absence of dramatic photon energy dependence for kz dispersion of

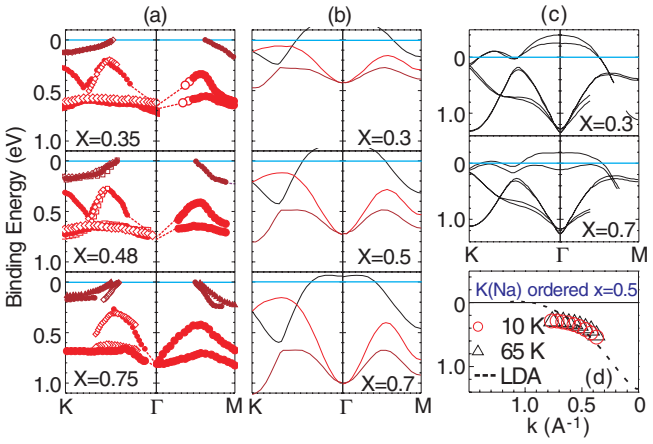

FIG. 3 (color online). Experiment versus theory: Comparison of (a) experimental band structures for $x = 0.35$, $x = 0.48$, and $x = 0.75$ with (b) LDA + large-U calculation [17] and (c) LAPW calculations [14]. (d) For sodium- or potassium-ordered samples, $x = 1/2$, the e_g' band is always below the Fermi level ($\sim$250 meV) at the temperature below or above insulating transition points.

the double band behavior observed in high doping ($x = 0.75$ or higher doping [11]) suggests the lack of three-dimensional coupling and points to a ferromagnetic or phase separated sample origin of the observed behavior.

We now compare our data with the calculations in [17] (Fig. 3). First, we note that all deeper-lying bands meet at the Γ point, consistent with theory and as expected on fundamental t_{2g} symmetry considerations. Second, a reasonable agreement is seen along the Γ-M cut in terms of the connectivity of the deeper-lying bands. Along the Γ-K cut, however, theory predicts a crossing between the upper e_g' band (e_{g1}) and the a_{1g} quasiparticle band. Our data suggest that this crossing is avoided at all dopings, and indicate a gap between the a_{1g} band and the upper e_g' band near $k \sim 0.55\pi$. Previously, this effect showed up only as a break in dispersion and was interpreted as a "kink" due to electron-phonon coupling [9,10]. In our high-quality data set it appears, instead, to resolve as a multiband hybridization effect [Fig. 3(a) (left)]. Our data suggest a strong mixing of the bands leading to an *anticrossing* behavior and the opening of a hybridization gap of magnitude more than 100 meV [Fig. 3(a) (left)]. This also suggests that the full quasiparticle band cannot be of pure a_{1g} symmetry.

We now consider the selection rules associated with e_g' and a_{1g} bands for different ARPES geometries. A symmetry analysis suggests that the e_{g1} states (based on the basis functions in LDA or DMFT [15]) near E_F and along the Γ-K cut are odd with respect to reflections about the plane formed by Γ-K and the normal of the Co plane. These e_{g1} states at E_F along Γ-K cannot possibly be observed using P-polarized geometry with coinciding planes of incidence and emission. The even a_{1g} and e_{g2} bands (the lower e_g' band) exhibit hybridization gaps. The odd e_{g1} band crosses these bands (a_{1g} and e_{g2}) without any interaction. For x along Γ-K and y along Γ-M, emission in the xz plane containing ΓK and P-polarized light incident in the same plane selection rules precludes any contribution from e_{g1} states since the final state is even in y. The detection geometry for the photoelectrons permits excitations only from a_{1g} and e_{g2} bands. Emission from e_{g1} states is allowed for the S-polarized light incident in the xz plane or the P-polarized light incident in the yz plane. Figures 4(a) and 4(b) show the experimental data along the Γ-M cut using P and S geometries, respectively. Only with the P geometry is strong emission detected near the Γ-M crossings. This is consistent with an a_{1g} character of the low-lying states along this cut. Figures 4(c) and 4(d) show the Γ-K cut using P and S geometries, respectively. The emission contrast is much less dramatic and the quasiparticle is only weakly enhanced under the P geometry.

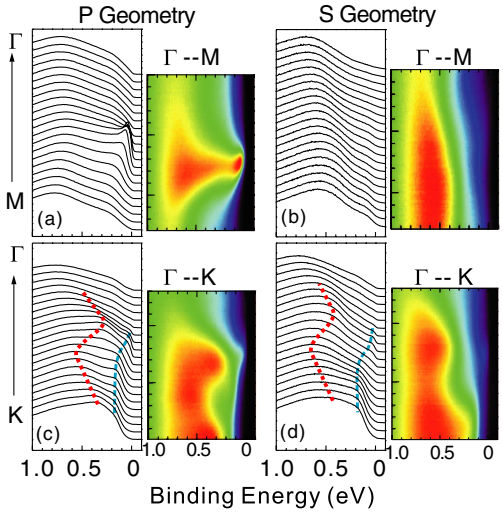

FIG. 4 (color online). Polarization dependence: The t_{2g} complex measured along the Γ-M and Γ-K cuts under P geometry (a),(c) and S geometry (b),(d). Red and blue (light and gray) dots trace the e_g' and a_{1g} bands, respectively. Geometries are defined in Figs. 1(c) and 1(d).

We note that LDA plus the multiorbital mean-field Hubbard model (LDA + large-U) can properly account for the sinking of the e_g' pockets and the suppression of the bandwidth at low Na doping near $x = 0.3$ [17]. Experiment suggests that a hybridization gap is also involved as suggested by Singh *et al.* [18].

Another mechanism that has been proposed for the sinking of the e_g' states is the effect of the random potential from the Na layer. This model suggests that the disordered sodium potential experienced by the heavy e_g' states leads to a localization of the carriers. We have studied the high-energy band structure of $(Na/K)_{1/2}CoO_2$ samples where Na or K ions order well above room temperature, thus removing the random potential which is experienced by the e_g' electrons at all other dopings. Experimentally, we find that while a_{1g} bands exhibit a gap of size less than 10 meV only at temperatures below the metal insulator transition (~51 K), the e_g' bands exhibit a clear gap well above the transition temperature and are located at about 250 meV below E_F [Fig. 3(d)] similar to what is seen at other dopings where Na ions are highly disordered.

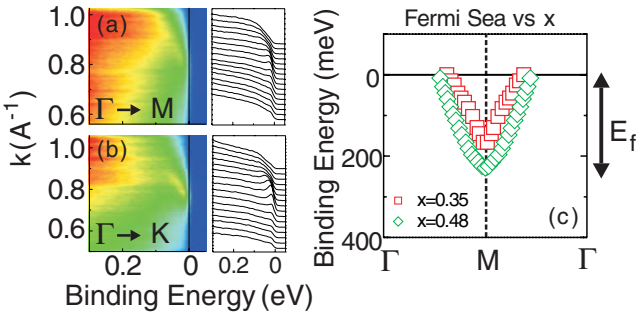

FIG. 5 (color online). Effect of hydration near $x = 1/3$: (a),(b) Fermi crossings are observed at 15 K in the hydrated $Na_xCoO_2 \cdot yH_2O$ compound near $x = 0.35$ while "y" varies from 0.7 to 1.4 (see text). (c) Quasiparticle bandwidth (many body E_F) is estimated from a complete dispersion relation measurement.

Therefore our results suggest that the sinking of the e_g' bands is not related to weak localization only. We further compare our data with linear augmented-plane-wave method (LAPW) calculations [14] in Fig. 3(c). LAPW results agree with our observation of a hybridization gap along Γ-K.

We have studied the effect of hydration on the low-lying electronic structure. Results are shown in Fig. 5. In comparison with unhydrated samples, our results suggest that hydration does not lead to any significant change in Fermi velocity. Under an unfavorable scenario where some H_2O is evaporated from top surface (unlikely to happen since experiments are carried out well below the freezing temperature of H_2O) a partial hydration effect is still probed in ARPES due to the buried nH_2O layers.

Our detailed systematic high-resolution measurements in the current study allow us to draw a direct connection with bulk-sensitive electronic density of states measurements. We note the average size of the Fermi surface $k_F \sim 0.77 \pm 0.05$ Å^{-1} and the velocity $\hbar v_F \sim 0.4 \pm 0.1$ eV Å for $x \sim 1/3$. Since the samples are mostly two dimensional in this doping range, the linear specific heat coefficient, γ, is set by k_F and v_F only as shown in [19–21]: $\gamma = [(\pi N_A k_B^2 a_o^2)/(3\hbar^2)] \sum m^*$, where $m^* = \hbar k_F / v_F$ (N_A is the Avogadro number, k_B is the Boltzman's constant, $\hbar$ is the Planck's constant, and a_o is the lattice constant), and $\gamma \sim 11.47 \pm 2.96$ mJ/mol K^2 ($a_o = 2.82$ Å).

This ARPES estimated value is close to that obtained with *bulk* thermodynamic measurements (~12.1 for unhydrated and 13.5 mJ/mol K^2 for the hydrated or the deuterated superconductors [22]). This leaves very little room for the six corner pockets to be shared, and if they exist, their sizes must be much smaller than the best k resolution of ARPES. Therefore, our data suggest that almost all of specific heat can be consistently explained with a single Fermi surface with a narrow renormalized band as we observe in this high-resolution work. This point is further supported by Shubnikov–de Haas data [19]. We also note that for $x = 0.75$ or higher dopings [11], ARPES data and specific heat data differ by more than a factor of 2. This discrepancy could be due to magnetic order on the top layer and/or intrinsic phase separation recently reported by several groups in these magnetic dopings [23]. This is the regime where 2D nonmagnetic Luttinger theorem was found to be not satisfied [11].

Finally, our systematic results allow us to estimate the bandwidth of the band that generates the FS in a clear fashion as shown in Fig. 5(e) since for the first time it can be traced over all of the BZ. The effective bandwidth of the occupied band that crosses the Fermi level is on the order of 0.25 eV. This is smaller than most other correlated oxide metals such as the cuprates, ruthenates or manganites [23,24].

In conclusion, we have measured the complete band dispersions in sodium cobaltates by utilizing the polarization and excitation-energy dependent matrix elements. A hybridization gap is observed along Γ-K which was previously interpreted as strong electron-phonon coupling. The extracted effective bandwidth, based on our complete dispersion measurements, is found to be smaller than most other similar correlated oxides. The measured ARPES density of states is found to be in agreement with the bulk electronic density of states measured in the specific heat and consistent with a single Fermi surface in the doping range where the 2D Luttinger theorem is fully satisfied in the ARPES data.

We acknowledge G. Khaliulin, G. Kotliar, B. Keimer, P. A. Lee, N. P. Ong, D. Singh, Z. Wang, and A. Fedorov for discussions. This work is primarily supported by DOE Grant No. DE-FG-02-05ER46200. R. J. C. acknowledges support by the NSF (DMR-0213706). N. L. W. acknowledges support by the NSFC (10574158).

*Electronic address: mzhasan@princeton.edu

[1] K. Takada *et al.*, Nature (London) **422**, 53 (2003).
[2] Y. Wang *et al.*, Nature (London) **425**, 423 (2003).
[3] M. Foo *et al.*, Phys. Rev. Lett. **92**, 247001 (2004).
[4] G. Baskaran, Phys. Rev. Lett. **91**, 097003 (2003).
[5] M. Mochizuki *et al.*, Phys. Rev. Lett. **94**, 147005 (2005).
[6] O. Motrunich and P. A. Lee, Phys. Rev. B **70**, 024514 (2004).
[7] I. I. Mazin *et al.*, Nature Phys. **1**, 91 (2005).
[8] J. Haerter *et al.*, cond-mat/0607293.
[9] M. Z. Hasan *et al.*, Phys. Rev. Lett. **92**, 246402 (2004).
[10] H. B. Yang *et al.*, Phys. Rev. Lett. **95**, 146401 (2005).
[11] D. Qian *et al.*, Phys. Rev. Lett. **96**, 216405 (2006).
[12] D. J. Singh, Phys. Rev. B **61**, 13 397 (2000).
[13] M. D. Johannes *et al.*, Phys. Rev. Lett. **93**, 097005 (2004).
[14] M. D. Johannes *et al.*, Europhys. Lett. **68**, 433 (2004).
[15] H. Ishida *et al.*, Phys. Rev. Lett. **94**, 196401 (2005).
[16] P. Zhang *et al.*, Phys. Rev. Lett. **93**, 236402 (2004); L.-J. Zou *et al.*, Phys. Rev. B **69**, 132505 (2004); K. W. Lee *et al.*, Phys. Rev. B **70**, 045104 (2004).
[17] S. Zhou *et al.*, Phys. Rev. Lett. **94**, 206401 (2005).
[18] D. J. Singh *et al.*, Phys. Rev. Lett. **97**, 016404 (2006).
[19] L. Balicas *et al.*, Phys. Rev. Lett. **97**, 126401 (2006).
[20] F. Baumberger *et al.*, Phys. Rev. Lett. **96**, 246402 (2006).
[21] C. Kittle, *Introduction to Solid State Physics* (Wiley, New York, 2005).
[22] R. Jin *et al.*, Phys. Rev. B **72**, 060512 (2005).
[23] C. de Vaulx *et al.*, Phys. Rev. Lett. **95**, 186405 (2005); M. Lee *et al.*, Nat. Mater. **5**, 537 (2006).
[24] E. W. Carlson *et al.*, in *The Physics of Conventional and Unconventional Superconductors*, edited by K. H. Bennemann and J. B. Ketterson (Springer-Verlag, Berlin, 2002).